ISSN 1674-1056
http://cpb.iphy.ac.cn
http://iopscience.iop.org/cpb
中国物理 B
Chinese Physics
中国物理 Chinese Physics B

Suppression of indium-composition fluctuations in InGaN epitaxial layers by periodically-pulsed mixture of N_2 and H_2 carrier gas

Hai-Long Wang(王海龙), Xiao-Han Zhang(张晓涵), Hong-Xia Wang(王红霞), Bin Li(黎斌), Chong Chen(陈冲), Yong-Xian Li(李永贤), Huan Yan(颜欢), Zhi-Sheng Wu(吴志盛), Hao Jiang(江灏)

Citation: Chin. Phys. B . 2018, 27(12): 127805. **doi:** 10.1088/1674-1056/27/12/127805
Journal homepage: http://cpb.iphy.ac.cn; http://iopscience.iop.org/cpb

What follows is a list of articles you may be interested in

N-type GaSb single crystals with high below-band gap transmission

Yong-Biao Bai(白永彪), You-Wen Zhao(赵有文), Gui-Ying Shen(沈桂英), Xiao-Yu Chen(陈晓玉), Jing-Ming Liu(刘京明), Hui Xie(谢晖), Zhi-Yuan Dong(董志远), Jun Yang(杨俊), Feng-Yun Yang(杨凤云), Feng-Hua Wang(王凤华)

Chin. Phys. B . 2017, 26(10): 107801. **doi:** 10.1088/1674-1056/26/10/107801

Enhancing redshift phenomenon in time-resolved photoluminescence spectra of AlGaN epilayer

Wei Li(李维), Peng Jin(金鹏), Wei-Ying Wang(王维颖), De-Feng Mao(毛德丰), Xu Pan(潘旭), Xiao-Liang Wang(王晓亮), Zhan-Guo Wang(王占国)

Chin. Phys. B . 2017, 26(7): 077802. **doi:** 10.1088/1674-1056/26/7/077802

Structural characterization of $Al_{0.55}Ga_{0.45}N$ epitaxial layer determined by high resolution x-ray diffraction and transmission electron microscopy

Qing-Jun Xu(徐庆君), Bin Liu(刘斌), Shi-Ying Zhang(张士英), Tao Tao(陶涛), Zi-Li Xie(谢自力), Xiang-Qian Xiu(修向前), Dun-Jun Chen(陈敦军), Peng Chen(陈鹏), Ping Han(韩平), Rong Zhang(张荣), You-Dou Zheng(郑有炓)

Chin. Phys. B . 2017, 26(4): 047801. **doi:** 10.1088/1674-1056/26/4/047801

Semipolar (1122) and polar (0001) InGaN grown on sapphire substrate by using pulsed metal organic chemical vapor deposition

Sheng-Rui Xu(许晟瑞), Ying Zhao(赵颖), Ren-Yuan Jiang(蒋仁渊), Teng Jiang(姜腾), Ze-Yang Ren(任泽阳), Jin-Cheng Zhang(张进成), Yue Hao(郝跃)

Chin. Phys. B . 2017, 26(2): 027801. **doi:** 10.1088/1674-1056/26/2/027801

High-efficiency InGaN/AlInGaN multiple quantum wells with lattice-matched AlInGaN superlattices barrier

Feng Xu(徐峰), Peng Chen(陈鹏), Fu-Long Jiang(蒋府龙), Ya-Yun Liu(刘亚云), Zi-Li Xie(谢自立), Xiang-Qian Xiu(修向前), Xue-Mei Hua(华雪梅), Yi Shi(施毅), Rong Zhang(张荣), You-Liao Zheng(郑有炓)

Chin. Phys. B . 2017, 26(1): 017803. **doi:** 10.1088/1674-1056/26/1/017803

Suppression of indium-composition fluctuations in InGaN epitaxial layers by periodically-pulsed mixture of N_2 and H_2 carrier gas*

Hai-Long Wang(王海龙), Xiao-Han Zhang(张晓涵), Hong-Xia Wang(王红霞), Bin Li(黎斌), Chong Chen(陈冲), Yong-Xian Li(李永贤), Huan Yan(颜欢), Zhi-Sheng Wu(吴志盛), and Hao Jiang(江灏)†

State Key Laboratory of Optoelectronic Materials and Technologies, Sun Yat-sen University, Guangzhou 510275, *China*

(Received 4 July 2018; revised manuscript received 16 September 2018; published online 10 November 2018)

Indium-composition fluctuations in InGaN epitaxial layers are suppressed by using periodically-pulsed mixture (PPM) of N_2 and H_2 carrier gas. Photoluminescence, optical transmission, reciprocal space map and space-resolved cathodoluminescence are employed to characterize the InGaN epilayers. It is shown that the lateral In-fluctuations mainly occur as hillock-like In-rich regions. Both the number and size of In-rich regions are reduced by introducing the PPM carrier gas. Moreover, the measurements first experimentally demonstrate that the H_2 carrier gas has a stronger decomposition effect on the In-rich region. As the duration time of the PPM carrier gas increases, the reduction of In-content in the In-rich region reaches up to 12%, however, only 2% for the In-homogeneous region. These factors lead to the suppression of In-fluctuations.

Keywords: InGaN alloys, suppression of In-fluctuations, periodically-pulsed mixture of nitrogen and hydrogen

PACS: 78.55.Cr, 81.05.Ea, 81.15.Gh **DOI:** 10.1088/1674-1056/27/12/127805

1. Introduction

InGaN ternary alloys are promising materials and have received enormous attention due to their direct and adjustable bandgaps in entire visible region, high theoretical electron mobility,[1] and large optical absorption.[2] These alloys offer many potential applications, such as quantum-well-based solid-state emitters,[3] light detectors, photovoltaics,[4] photoelectrochemical (PEC),[5] and thermoelectric devices.[6] For some applications, such as visible light detectors and solar cells, an InGaN film with thickness in excess of 100 nm is required to absorb more than 90% of the incident above-bandgap light.[7] However, due to the low miscibility[8] and large difference in interatomic spacing between GaN and InN ($\sim$ 11%),[9,10] Indium-composition fluctuations (In-fluctuations) occur easily in InGaN epitaxial layers and result in poor electrical and structural properties, especially for high In-content. Moreover, InGaN epilayers which are generally deposited on GaN buffer layer suffer a large lattice constant mismatch between InGaN and GaN and a small critical layer thickness (CLT). For example, The CLT of an $In_xGa_{1-x}N$ epilayer with $x > 10\%$ is calculated to be less than 100 nm.[11] When the thickness of InGaN epilayer exceeds the CLT, strain relaxation accompanied by the formation of dislocations may occur. Therefore, it is difficult to prepare high crystalline quality InGaN epilayers with In-content $> 10\%$ and thickness > 100 nm due to the severe In-fluctuations and high defect density.[12]

Up to now, some efforts have been made to suppress the In-fluctuations in InGaN and these efforts can be classified, in essence, as three categories: (i) strain control, it was proposed that elastic strain helps to suppress the In-fluctuations in InGaN,[9] and single-phase InGaN layers have been grown on lattice-matched ZnO substrates through compressive strain;[13] (ii) non-equilibrium growth, it was found that In-fluctuations could be suppressed by promoting growth rate, thereby converting thermodynamic conditions into non-equilibrium growth conditions;[14] and (iii) indium adlayer control, including semi-bulk methods,[7,15,16] metal-modulated epitaxy,[17,18] and indium modulation technology.[19] All these epitaxial methods use pure nitrogen as carrier gas. It is worth noting that hydrogen was often adopted as carrier gas during the growth of barriers[20,21] and the interruptions between barriers and wells in InGaN multiple quantum wells (MQWs).[22] Its effects have been studied for at least 20 years and one of the effects was that hydrogen could eliminate the inclusions, namely In-fluctuations.[20–22] For thick InGaN epitaxial layers, some investigations have been done about the effects of hydrogen on indium incorporation[23,24] and C and O impurities.[25] However, there are few reports on the effects of hydrogen on the In-fluctuations in thick InGaN layers.

In the present work, we provide another method to suppress the In-fluctuations during the growth of thick InGaN layers by periodically-pulsed mixture (PPM) of N_2 and H_2 carrier gases. In-rich regions, which mainly contribute to the In-fluctuations, are directly observed and evidently reduced by

*Project supported by the Science and Technology Major Project of Guangdong Province, China (Grant No. 2015B010112001) and the Natural Science Foundation of Guangdong Province, China (Grant No. 2015A030312011).

†Corresponding author. E-mail: stsjiang@mail.sysu.edu.cn

© 2018 Chinese Physical Society and IOP Publishing Ltd

the PPM carrier gas. The effects of hydrogen on the In-rich region and In-homogeneous region are first experimentally investigated. It is shown that hydrogen has much stronger decomposition effect on the In-rich regions and, therefore, the In-fluctuations can be effectively suppressed by controlling the duration time of PPM.

2. Experiments

All experimental InGaN samples were grown on *c*-plane sapphire substrates by low-pressure metal–organic chemical vapor deposition (MOCVD) in a closed-coupled showerhead reactor. Trimethyl indium (TMIn), tetraethyl gallium (TEGa), and ammonia (NH_3) were used as metal and nitride precursors, respectively. N_2 or H_2 carrier gas flowed through the metal precursors bubblers. The growth temperature measured by pyrometer was converted into the wafer temperature shown here, calibrated by means of the blackbody radiation. The substrate temperature was firstly increased to 1098 °C in H_2 atmosphere for 300 s to remove the surface damage and contamination. Then, a 30-nm-thick GaN nucleation layer was grown at 536 °C, followed by a 2.5-μm-thick unintentionally doped (uid) GaN layer deposited at 1069 °C. Next, an $In_xGa_{1-x}N$ (x ∼ 14%) transition layer with nominal 60-nm thickness was grown with pure N_2 carrier gas to avoid aggravating the composition pulling effect. Finally, a uid-InGaN main layer with nominal 90-nm thickness was deposited under the identical growth conditions of transition layer except for the periodically changed carrier gas between pure N_2 gas and a mixed gas of H_2 (400 sccm) and N_2 (5842 sccm). During the deposition of all InGaN layers, the metal and nitride precursors were kept continuous. The flow rate of NH_3, TMIn, and TEGa were 9 slm, 27.72 μmol/min, and 4.52 μmol/min, while the growth temperature and pressure were 765 °C and 300 mbar (1 bar = 10^5 Pa), respectively. Four samples were grown by PPM method with pulsed duration times of 0, 5, 10, and 15 s in each period of 45 s, respectively. The InGaN main layer consists of 55 periods in total and each periodic thickness is around 1.6 nm, corresponding to the growth rate of ∼ 2.2 nm/min. It should be noted that there were no multilayered structures observed in InGaN main layers by transmission electron microscopy, indicating that the deposited InGaN should be bulk film rather than superlattice. The flow sequences of the carrier gas during the growth of InGaN main layer are shown in the inset of Fig. 1. Photoluminescence (PL) measurements were performed at room temperature by using a He–Cd laser operating at 325 nm. Optical transmission spectra were recorded with a Shimadzu UV 2550 UV-VIS Spectrophotometer. Space-resolved cathodoluminescence (CL) images were obtained by using MonoCL4 system, where surface morphology can be imaged via secondary electrons simultaneously with the monochromatic CL intensity distribution. The acceleration voltage of electron beam was operated at 2 kV for the sake of focusing electron beam on the InGaN main layers. High resolution x-ray diffraction (HRXRD) and reciprocal space map (RSM) measurements were carried out by using a Bruker D8 discovery instrument. Atomic force microscopy (AFM) was conducted in tapping mode on a Veeco Dimension Edge system. Fresh tip was utilized to obtain the reliable and clear surface morphology.

3. Results and discussion

Figure 1 shows the room-temperature PL spectra. No obvious In-fluctuations can be observed from the spectra. As the duration time of PPM increases from 0 s to 10 s, the main PL peak position slightly shifts from 436 nm to 424 nm with the increase of peak intensity. This blue-shift is caused by the introduction of H_2 carrier gas, which impedes the In-incorporation. The increased integrated PL intensity of 183% indicates a reduction of non-radiative recombination centers which trap the photo-generated carriers and degrade optoelectronic performance.[26] When the duration time increases to 15 s, the peak wavelength of InGaN main layer significantly decreases to 412 nm, resulting in a significant blue-shift of 24 nm with respect to the 0-s sample. The large blue shift of PL peak indicates that the 15-s duration time is too long to avoid reducing the In-content and, therefore, the 15-s sample is not further considered in the discussion. The PL peak wavelengths and corresponding In-content of these three samples are listed in Table 1. Each of the PL spectra also

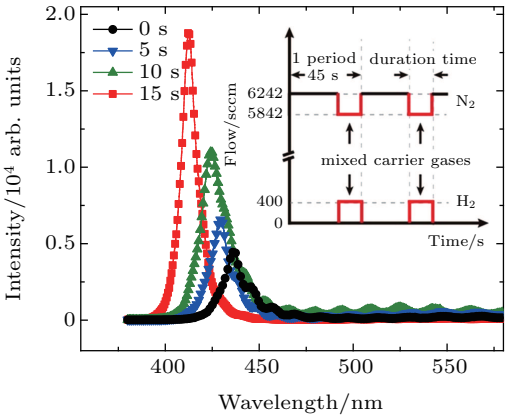


Fig. 1. (color online) PL spectra with inset showing carrier gas flow sequences, where partial nitrogen is replaced by hydrogen during mixture duration time. All metal and nitride precursors are kept constant, respectively.

Table 1. PL peak wavelengths and corresponding In-content calculated by modified Brunner method[28] for samples with mixture duration times of 0 s, 5 s, 10 s, and 15 s, respectively.

Sample	0 s	5 s	10 s	15 s
λ/nm	436	429	424	412
In-content	0.14	0.13	0.12	0.10

exhibits a very weak emission around 525 nm. However, the peak position and line shape cannot be precisely determined due to the oscillations caused by the interference effect appearing usually in InGaN layers.[11,27]

Figure 2 shows the optical transmission spectra of the three samples. By increasing the duration time, the main absorption edge of InGaN around 425 nm is slightly blue-shifted. This is consistent with the PL measurement. The spectra in the long wavelength region are modulated by an interference effect and appear with many fringes. According to the method described in Ref. [29], the thickness of epitaxial layer can be evaluated from the interference fringes. The consequently obtained result is ~ 2.5 μm, roughly equaling the total thickness of epitaxial layers. This implies that the interference effect occurs at the InGaN surface and the interface between sapphire and GaN which is due to the comparative refractive indexes of GaN and InGaN. The interference effect appearing in the transmission spectra also reflects good thickness uniformity and high InGaN surface quality.[29] To clearly compare the transmission spectra in the long wavelength region beyond the band edge, we plot the geometric mean T_α of upper transmission envelope T_M and lower transmission envelope T_m in the inset of Fig. 2, in which $T_\alpha = (T_\mathrm{M} \cdot T_\mathrm{m})^{1/2}$ as described in Ref. [30]. According to the obtained T_α curves, the transmission spectra can be divided into two regions; *i.e.*, the transparent region beyond 672 nm and the weak-absorption region lying approximately between 450 nm and 672 nm. In the transparent region, T_α values keep almost constant for the three samples, while in the weak-absorption region the T_α values decrease with wavelength decreasing and increase with PPM duration time increasing. The reduction of T_α might be ascribed to the inhomogeneous In-rich components, which was also reported by Chen *et al.*[31] This means that the increase of PPM duration time may lead to an effective reduction of the In-rich components in the InGaN epilayers. However, because the optical transmittance is also related to the surface scattering and the impurity absorption, more proofs are needed to confirm the above analysis.

To further investigate the effects of PPM carrier gas on the deposited InGaN, we also carry out space-resolved CL measurements. The measured results are shown in Fig. 3. Figures 3(a)–3(c) exhibit the scanning electron microscopic (SEM) images. Figures 3(d)–3(f) show the monochromatic CL images dealt with mixed colour technology. Figures 3(g)–3(i) display the CL spectra of the samples with the duration times of 0 s, 5 s, and 10 s, respectively. For the 0-s sample, many hillocks with the dimensions of several microns can be observed in the SEM image as shown in Fig. 3(a). These hillocks have irregular shapes and distributed randomly on the InGaN surface. The CL image (Fig. 3(d)) shows that the hillocks present the spatially inhomogeneous luminescence of InGaN epilayer. The luminescence measured from the central regions of hillocks (red areas) show an emission band ranging from 520 nm to 650 nm, while that from the marginal areas of hillocks (green areas) exhibits a band ranging from 460 nm to 500 nm. For the blue areas, the emission band is relatively narrow which ranges from 420 nm to 450 nm. These areas in 0-s sample correspond to the In-homogeneous regions with a PL emission peak of 436 nm. The CL images reveal a fact that the closer to the centre of hillocks, the longer the emission wavelength is. These hillocks are In-rich regions which are the main contribution to the lateral In-fluctuations of InGaN. Comparing with 0-s sample and 5-s sample, it can be found that both the number and size of the hillocks significantly decrease in the 10-s sample, which indicates that the introduction of PPM carrier gas effectively suppresses the In-rich region in the InGaN epilayer.

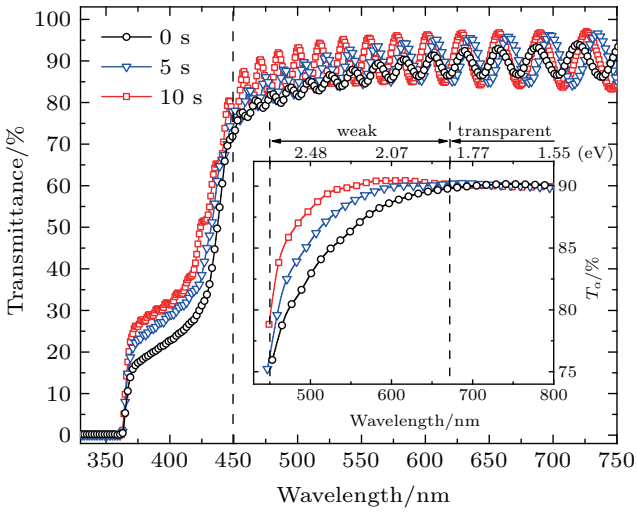


Fig. 2. (color online) Optical transmittance curves with inset showing geometric mean transmission spectra.

Besides the number and size of the hillocks, the variation of CL spectrum with the PPM duration time is also important for understanding the role of PPM carrier gas. The CL spectra are therefore characterized by focusing an electron beam on the selected hillocks, as shown in Figs. 3(g)–3(i). For the 0-s sample, the CL emission peak of an In-rich region (point A) is ~ 677 nm (denoted as peak #1), corresponding to an In-content of $\sim 49\%$; while the emission peak of the In-homogeneous region is in agreement with the PL peak result (not shown here) and the In-content is calculated to be $\sim 14\%$. This indicates that the lateral In-fluctuations are much more serious in this sample. As the PPM duration time increases to 5 s, another emission peak around 567 nm (marked as peak #2) is measured from an In-rich region of point B. The corresponding In-content is $\sim 37\%$. Further increasing the duration

time to 10 s leads emission peak #1 to disappear and emission peak #2 to still exist as shown in the CL spectrum taken from an In-rich region of point C. These observations confirm that not only the size and number but also the In-content of In-rich regions can be effectively reduced by the PPM carrier gas, or specifically the H_2 carrier gas. Comparing with the In-homogeneous regions (only $\sim 2\%$), the In-content decreases more evidently in the In-rich region (up to $\sim 12\%$), which means that the effect of H_2 carrier gas on the In-rich InGaN region is very effective. Therefore, better result is expected to be achieved by further optimizing the flow ratio between H_2 and N_2 carrier gas and the duration time of pulse flow.

It should be noted that the spatial extent of In phase separation is still under debate.[32–34] However, the dimension of the phase separation is typically on the order of a few to tens of nanometres, much smaller than the sizes of inhomogeneous regions observed in our InGaN epitaxial layers. Accordingly, strictly speaking, the effect of PPM carrier gas shown in our case is to suppress the In-composition fluctuations rather than the phase separation. The above analysis therefore demonstrates that the suppression of In-fluctuations is a major contribution of the PPM carrier gas.

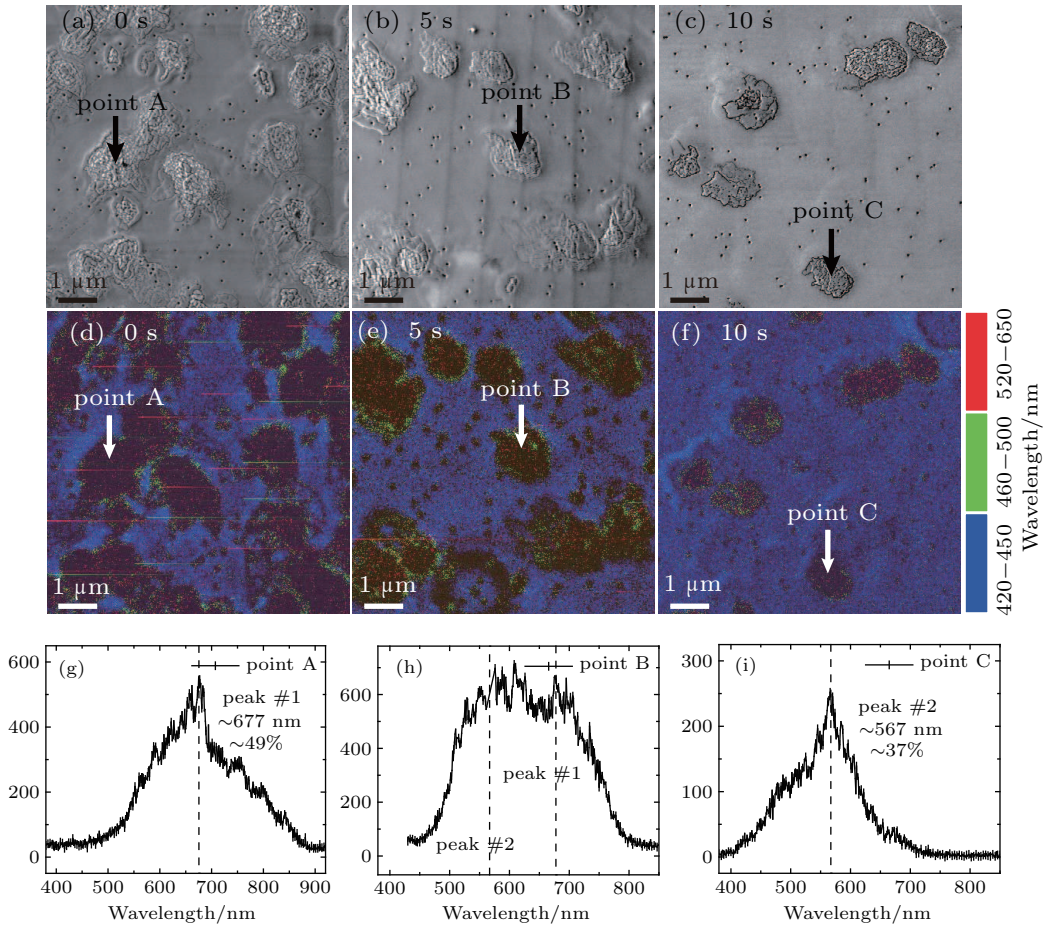


Fig. 3. (color online) (a)–(c) SEM images; (d)–(f) monochromatic CL images; (g)–(i) CL spectra of samples with the duration times of 0 s, 5 s, and 10 s, respectively.

The hydrogen in PPM carrier gas plays an important role in suppressing the In-fluctuations during the InGaN epitaxy by the MOCVD method. On the one hand, hydrogen could etch (or decompose) InN more easily than GaN via the reverse synthesis reaction because of its small equilibrium constant.[35,36] Indium, one of the reverse synthetic products, partially reacts with hydrogen and forms indium-hydride volatile species[37] which could be desorbed seriously due to their weaker bonds to the surface than In atoms.[4] Meanwhile, hydrogen is a by-product of deposition reactions of $\mathrm{In}\,(g)+\mathrm{NH_3}\,(g)=\mathrm{InN}\,(s)+\frac{3}{2}\mathrm{H_2}(g)$ and $\mathrm{Ga}\,(g)+\mathrm{NH_3}\,(g)=\mathrm{GaN}\,(s)+\frac{3}{2}\mathrm{H_2}(g)$. The introduction of H_2 carrier gas increases the hydrogen partial pressure and prevents the synthesis of InN, and thus impeding the generation of the In-rich regions. These two factors contribute to the effects of hydrogen on the In-rich regions and the consequent suppression of In-fluctuations, which may also lead to a slight decrease of In-incorporation into the In-homogeneous region.

The RSM measurements of asymmetric (105) reflection are performed to further clarify the mechanism of In-fluctuation suppression from the aspect of strain conditions. The broad diffraction spot shown in Fig. 4(a) indicates a dispersive distribution of In-composition and strain in the InGaN epilayer of 0-s sample. With the introduction of PPM carrier

gas, another diffraction peak of InGaN appears with larger Q_z value, as shown in Figs. 4(b) and 4(c). Note that all of these samples have identical GaN buffer layer and InGaN transition layers, the only difference is the InGaN main layer grown with a different PPM carrier gas. A slight decrease in In-content of the InGaN main layer is proven by the PL spectra as the PPM duration time increases. The appearing of diffraction peak is therefore attributed to the InGaN main layer. Moreover, the diffraction spots of InGaN main layers become relatively narrow, suggesting a more uniform In-composition and concentrated strain distribution. The degree of relaxation is defined as

$$R = \frac{a(L) - a_0(s)}{a_0(L) - a_0(s)}, \tag{1}$$

where a(L) and a_0(L) are the measured and fully relaxed in-plane lattice constants of InGaN layer, respectively, and $a_0(s)$ is the in-plane lattice constant of fully relaxed GaN. The fully strained line ($R = 0$) and relaxed line ($R = 1$) are depicted in Fig. 4. For the 0-s sample, a small horizontal shift of InGaN diffraction maximum with respect to that of GaN can be observed, meaning a partial in-plane relaxation; while there is nearly no diffraction maximum shift between InGaN and GaN for 10-s sample. The relaxation degrees of 0-s and 5-s samples are calculated to be 6% and 5%, respectively, according to the model described in Ref. [38]. When the duration time increases to 10 s, a small relaxation degree is obtained to be 1%. The almost full strain has two positive effects: (i) it is useful to suppress In-fluctuations in InGaN due to elastic strain;[9] (ii) and as the strain relaxation is usually accompanied by the formation of dislocations,[11] the threading defects can be reduced by maintaining the compressive strain. In fact, it is found that for the 10-s sample, the full width at half maximum (FWHM) of InGaN (002) and (102) rocking curves are 306 arcsec and 476 arcsec, respectively, much lower than those of 0-s sample (410 arcsec and 749 arcsec, respectively). This is also proven by SEM images (shown in Fig. 3), where the density of V-pits decreases with mixture duration time increasing. These reductions illustrate the improved InGaN crystalline quality.

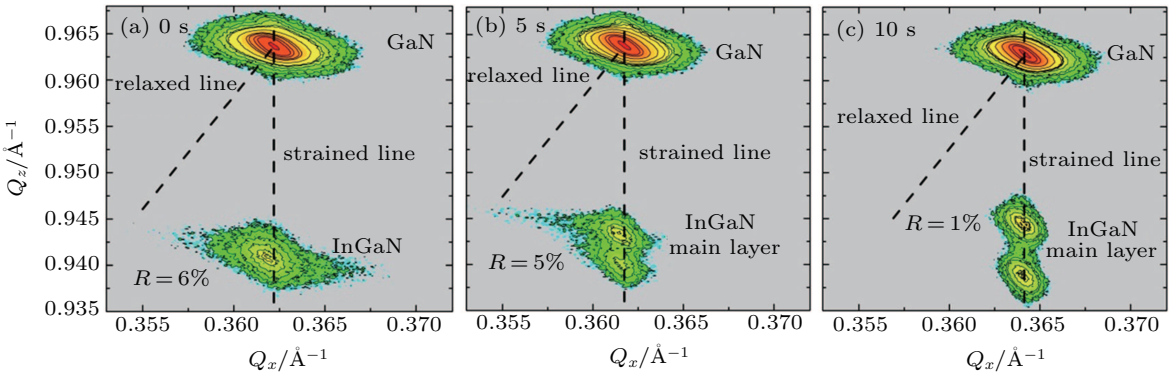


Fig. 4. (color online) (105) RSMs of samples with duration times of (a) 0 s, (b) 5 s, and (c) 10 s. Relaxed line and strained line are plotted.

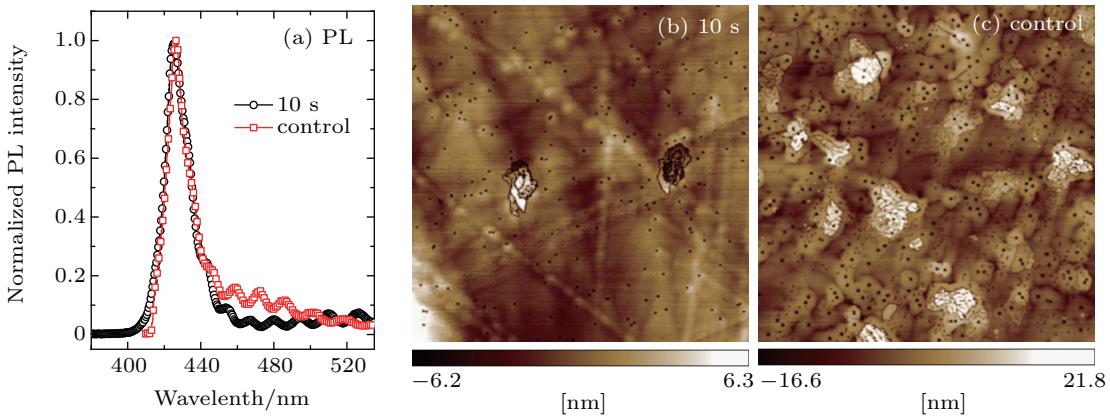


Fig. 5. (color online) (a) PL spectra, (b) AFM image (10 μm×10 μm) of the 10-s sample, and (c) control sample which is deposited under N_2 carrier gas.

Since the PPM carrier gases may also result in the decrease of In-content in InGaN layer, it is still necessary to clarify the effect of In-content reduction on In fluctuation. An InGaN control sample deposited with N_2 carrier gas is prepared. Figure 5(a) shows the PL spectrum of the 10-s and control sample. The emission peaks are observed at 425 nm and 426 nm for the 10-s and control samples respectively, indicating that the two InGaN samples have a similar In content value of $\sim$ 12%. Furthermore, another weak emission band at around 450 nm–500 nm appears only for the control

sample. Figures 5(b) and 5(c) show AFM images of the 10-s and control samples, respectively. Two hillock-like regions are observed in the 10-s sample and demonstrated to be In-rich InGaN regions by the space-resolved CL (Fig. 3). For the control sample, much more hillock-like regions with large sizes are characterized, implying more serious In-fluctuations in the control sample. These hillock-like regions also result in a rough surface morphology with a root mean square (rms) value of 4.74 nm, while the rms value is only 1.54 nm for the 10-s sample. These results suggest that the suppression of In fluctuations in this work is attributed to the PPM carrier gas rather than the In-content reduction.

4. Conclusions

In this work, a periodically-pulsed mixture of N_2 and H_2 carrier gas is introduced into the MOCVD during InGaN growth. The In-fluctuations are effectively suppressed by this method. A decreasing process of In-content in the In-rich region with increasing the hydrogen duration time is first clearly presented. It is found that not only the number and size of the hillock-like In-rich InGaN regions but also the In-content of the In-rich region is significantly reduced by the introduction of PPM carrier gas. These factors contribute to the suppression of In-fluctuations. The PPM carrier gas provides a way to precisely control the reaction amount and time of introduced hydrogen.

References

[1] Chin V W L, Zhou B, Tansley T L and Li X 1995 *J. Appl. Phys.* **77** 6064

[2] Bae S Y, Song Y H, Jeon S R, Kim D M, Jho Y D and Lee D S 2014 *J. Cryst. Growth* **387** 23

[3] Tong J H, Li S T, Lu T P, Liu C, Wang H L, Wu L J, Zhao B J, Wang X F and Chen X 2012 *Chin. Phys. B* **21** 118502

[4] Czernecki R, Kret S, Kempisty P, Grzanka E, Plesiewicz J, Targowski G, Grzanka S, Bilska M, Smalc-Koziorowska M, Krukowski S, Suski T, Perlin P and Leszczynski M 2014 *J. Cryst. Growth* **402** 330

[5] Gokarna A, Gauthier-Brun A, Liu W, Androussi Y, Dumont E, Dogheche E, Teng J H, Chua S J and Decoster D 2010 *Appl. Phys. Lett.* **96** 191909

[6] Pantha B N, Dahal R, Li J, Lin J Y, Jiang H X and Pomrenke G 2008 *Appl. Phys. Lett.* **92** 042112

[7] Gmili Y E, Orsal G, Pantzas K, Moudakir T, Sundaram S, Patriarche G, Hester J, Ahaitouf A, Salvestrini J P and Ougazzaden A 2013 *Acta Mater.* **61** 6587

[8] Pantha B N, Li J, Lin J Y and Jiang H X 2008 *Appl. Phys. Lett.* **93** 182107

[9] Karpov S Y 1998 *MRS Internet J. Nitride Semicond. Res.* **3** 16

[10] El-Masry N A, Piner E L, Liu S X and Bedair S M 1998 *Appl. Phys. Lett.* **72** 40

[11] Kang J H, Ebaid M, Lee J K and Ryu S W 2015 *Appl. Phys. A* **121** 765

[12] Ozaki T, Takagi Y, Nishinaka J, Funato M and Kawakami Y 2014 *Appl. Phys. Express* **7** 091001

[13] Li N, Wang S J, Park E H, Feng Z C, Tsai H L, Yang J R and Ferguson I 2009 *J. Cryst. Growth* **311** 4628

[14] Pantha B N, Li J, Lin J Y and Jiang H X 2010 *Appl. Phys. Lett.* **96** 232105

[15] Pantzas K, Gmili Y E, Dickerson J, Gautier S, Largeau L, Mauguin O, Patriarche G, Suresh S, Moudakir T, Bishop C, Ahaitouf A, Rivera T, Tanguy C, Voss P L and Ougazzaden A 2013 *J. Cryst. Growth* **370** 57

[16] Pantzas K, Patriarche G, Troadec D, Kociak M, Cherkashin N, Hytch M, Barjon J, Tanguy C, Rivera T, Suresh S and Ougazzaden A 2015 *J. Appl. Phys.* **117** 055705

[17] Moseley M, Lowder J, Billingsley D and Doolittle W A 2010 *Appl. Phys. Lett.* **97** 191902

[18] Moseley M, Gunning B, Greenlee J, Lowder J, Namkoong G and Doolittle W A 2012 *J. Appl. Phys.* **112** 014909

[19] Woo H, Jo H, Kim J, Cho S, Jo Y, Roh C H, Lee J H, Seo Y, Park J, Kim H, Hahn C K and Im H 2017 *Curr. Appl. Phys.* **17** 1142

[20] Suihkonen S, Lang T, Svensk O, Sormunen J, Torma P T, Sopanen M, Lipsanen H, Odnoblyudov M A and Bougrov V E 2007 *J. Crysl. Growth* **300** 324

[21] Ting S M, Ramer J C, Florescu D I, Merai V N, Albert B E, Parekh A, Lee D S, Lu D, Christini D V, Liu L and Armour E A 2003 *J. Appl. Phys.* **94** 1461

[22] Moon Y T, Kim D J, Song K M, Choi C J, Han S H, Seong T Y and Park S J 2001 *J. Appl. Phys.* **89** 6514

[23] Piner E L, Behbehani M K, El-Masry N A, Mclntosh F G, Roberts J C, Boutros K S and Bedair S M 1997 *Appl. Phys. Lett.* **70** 461

[24] Bosi M and Fornari R 2004 *J. Cryst. Growth* **265** 434

[25] Piner E L, Behbehani M K, El-Masry N A, Roberts J C, Mclntosh F G and Bedair S M 1997 *Appl. Phys. Lett.* **71** 2023

[26] Sumiya M, Toyomitsu N, Nakano Y, Wang J, Harada Y, Sang L, Sekiguchi T, Yamaguchi T and Honda T 2017 *APL Mater.* **5** 016105

[27] Namvar E and Fattahi M 2008 *J. Lumin.* **128** 155

[28] Laws G M, Larkins E C, Harrison I, Molloy C and Someford D 2001 *J. Appl. Phys.* **89** 1108

[29] Swanepoel R 1983 *J. Phys. E: Sci. Instrum.* **16** 1214

[30] Marquez E, Ramirez-Malo J, Villares P, Jimenez-Garay R, Ewen P J S and Owen A E 1992 *J. Phys. D: Appl. Phys.* **25** 535

[31] Chen Z Z, Qin Z X, Hu X D, Yu T J, Yang Z J, Tong Y Z, Ding X M and Zhang G Y 2004 *Physica B* **344** 292

[32] Dobrovolskas D, Mickevicius J, Nargelas S, Vaitkevicius A, Nanishi Y, Araki T and Tamulaitis G 2017 *Semicond. Sci. Technol.* **32** 025012

[33] Tao T, Zhi T, Liu B, Li Y, Zhuang Z, Xie Z, Chen D, Chen P, Zhang R and Zheng Y 2014 *Phys. Status Solidi A* **211** 2823

[34] Liu J, Liang H, Xia X, Liu Y, Liu J, Abbas Q, Shen R, Luo Y, Zhang Y and Du G 2017 *Cryst. Growth* **17** 3411

[35] Kryzhanovskaya N V, Lundin W V, Nikolaev A E, Tsatsulnikov A F, Sakharov A V, Pavlov M M, Cherkachin N A, Hytch M J, Valkovsky G A, Yagovkina M A and Usov S O 2010 *Semiconductors* **44** 828

[36] Koukitu A, Taki T, Takahashi N and Seki H 1999 *J. Cryst. Growth* **197** 99

[37] Koleske D D, Wierer Jr J J, Fischer A J and Lee S R 2014 *J. Cryst. Growth* **390** 38

[38] Pereira S, Correia M R, Pereira E, O'Donnell K P, Alves E, Sequeira A D, Francol N, Watson M and Deatcher C J 2002 *Appl. Phys. Lett.* **80** 3913